Electronic Supplementary Information

Elucidating the restructuring-induced highly active bimetallic Pt-Co/KL catalyst for *n*-heptane aromatization

Shuyuan Wang[a,d], Dan Xu[b,*], Di Zhu[b], Baofeng Zhao[b], Haibin Guan[b], Yong Qin[a,*], Baoshan Wu[a,c,*], Yong Yang[a,c], Yongwang Li[a,c]

[a] State Key Laboratory of Coal Conversion, Institute of Coal Chemistry, Chinese Academy of Sciences, Taiyuan 030001, People's Republic of China

[b] Energy Research Institute, Qilu University of Technology (Shandong Academy of Sciences), Jinan, 250014, People's Republic of China

[c] National Energy Research Center for Clean Fuels, Synfuels China Co., Ltd, Beijing 101400, People's Republic of China

[d] University of Chinese Academy of Sciences, Beijing 100049, People's Republic of China

*Corresponding authors: xudan@sderi.cn, qinyong@sxicc.ac.cn, wbs@sxicc.ac.cn

1. Experimental details

2. List of Figures

3. List of Tables

1. Experimental details

1.1. Catalyst preparation

The PtCo-n/KL catalysts with different Pt and Co cycle numbers were synthesized by ALD method. Typically, ALD was performed in a homemade closed chamber-type reactor at 300 ^{o}C with the N_2 used as carrier gas (50 mL/min). Trimethyl(methylcyclopentadienyl)platinum ($MeCpPtMe_3$) and cobaltocene ($CoCp_2$) were used as the precursors of Pt and Co, respectively. $MeCpPtMe_3$ was kept at 60 ^{o}C and $CoCp_2$ was heated to 70 ^{o}C to obtain enough vapor pressure. Ozone (O_3) was used as oxidizing agent. Prior to ALD, KL zeolite was dispersed in ethanol and then dropped onto a quartz wafer. The deposition of Pt was performed by sequential exposure of the KL zeolite to $MeCpPtMe_3$ and O_3, respectively. The pulse, exposure and purge times were 0.5, 300 and 100 s for $MeCpPtMe_3$ and 1, 100 and 40 s for O_3. For Co deposition, the pulse, exposure and purge times were 2, 8, 20 s for $CoCP_2$ and 1, 8 and 20 s for O_3. The obtained samples with five Pt ALD cycles and different Co ALD cycle numbers were labeled as PtCo-n/KL (n = 1, 5, 20), where *n* represents the ALD cycle numbers of Co. In these catalysts, the Pt was deposited on the KL support with five cycles firstly, the Co was deposited with the variety of cycles (1, 5, 20) secondly. For comparison, the CoPt/KL catalyst was synthesized by depositing Co with five cycles firstly and Pt with five cycles secondly. In addition, the monometallic Pt/KL and Co/KL catalysts with five cycles were also prepared in the similar method.

1.2. Catalyst characterizations

The microspore surface areas and volumes of catalysts were determined by N_2-adsorption measurements using ASAP 2020 equipment (Micromeritics, USA). The X-ray power diffraction patterns were collected on a Bruker D8 Advance X-ray laboratory diffractometer using Cu Kα (30 kV, 10mA). The content of the Pt and Co was determined by inductively coupled plasma-atomic emission spectrometer (Optima 2100DV, Perkin-Elmer).

Scanning electron microscope (SEM) was performed on the FEI QUANTA 400. High angle annular dark field scanning transmission electron microcopy (HAADF-STEM) measurement was conducted at FEI Talos^{TM} 200A and JEOL ARM 200F high-resolution microscopy operating at 200 kV. X-ray photoelectron spectroscopy (XPS) was recorded with a Physical Electronics Company

Quantum-2000 scanning ESCA microprobe with monochromatic Al K_α radiation. Prior to measurement, the samples were in situ reduced in an H_2 at 500 °C for 2 h. All binding energy values were corrected to C1s peak at 284.8 eV.

Diffuse reflectance infrared Fourier transform spectroscopy (DRIFTS) of CO adsorbed on the samples was conducted at a VERTEX70 spectrometer (Bruker, Germany). The catalyst was reduced at 500 °C for 1 h under a H_2 flow (99.9992%, 20 mL/min). Subsequently, the sample was purged with He (99.9992%, 20 mL/min) for 30 min at 500 °C and cooled to 40 °C. Then switch to 10% CO/He (20 mL/min) for 30 min, and subsequent purging with He to remove CO from the gas phase. Then the spectrum of adsorbed CO was collected during CO adsorption and following the He purge. In situ Fourier transform infrared (FT-IR) spectra of hydrocarbon species adsorption were recorded using an EQUINOX 70 (Bruker, Germany) apparatus under infrared transmission-absorption model. Before measurement, the sample was first located in situ reaction tank and reduced in H_2 flow at 500 °C for 1 h, then the sample was cooled in H_2 flow to 420 °C. When the vacuum degree of the reaction tank dropped to 10^{-4} Pa, the *n*-heptane steam was pulse into the reaction tank for 30 s, then the H_2 flow was continuously exposed to the reaction tank for 20 min. After that, the reaction tank was evacuated until the vacuum degree reached 10^{-4} Pa, then the *n*-heptane and H_2 flow was exposed again with various times. The spectrum was collected during the whole process. The spent catalysts with different reaction times (20-400 min) were removed to the VERTEX70 spectrometer for the IR measurement of CO adsorption according to the above description method.

1.3. Catalytic evaluation

The aromatization of *n*-heptane was performed in a stainless steel fixed-bed reactor at atmospheric pressure with a hydrogen/*n*-heptane molar ratio of 6 and WHSV = 0.68 h^{-1}. In a typical procedure, 300 mg catalyst (40-60 mesh) was loaded into the reactor and the silica sand at both sides of catalysts was employed. Prior to reaction, the catalyst was heated to 500 °C in flowing H_2 (20 mL/min) and kept for 1 h. When the temperature decreased to reaction temperature (420 °C), *n*-heptane was continuously pumped into the reactor. The products were analyzed by on-line gas chromatography (Agilent 7980A) equipped with a TCD detector and two FID detectors. The carbon balance was typically better than 95%.

Kinetic studies were performed in the same fixed-bed reactor and the conversion of *n*-heptane was kept below 15 % with the reaction temperature varied in the range of 340-420 ^{o}C. The apparent activation energy values were determined by the Arrhenius equation. Mears' criterion (C_M) was used to check the absence of heat transfer. The Mears' criterion (C_{MR}) and Weisz-Prater criterion (C_{WP}) were employed to confirm the absence of external and internal diffusion, respectively.

1.4. DFT calculation

DFT calculations were implemented in the Vienna Ab initio Simulation Package (VASP, 5.4.1).[1, 2] The electron-ion interaction was described with the projector augmented wave (PAW).[3, 4] The electron-exchange and correlation energies were treated within the generalized gradient approximation and the Perdew-Burke-Ernzerhof (GGA-PBE) functional.[5] The cutoff in the plane-wave basis was 400 eV. The adsorption energy (E_{ad}) was defined as follows: $E_{ad} = E_{M/slab} - (E_{slab} + E_M)$. Where $E_{M/slab}$ is the total energy of the slab with adsorbate, the E_{slab} is the energy of the slab and E_M is the total energy of the adsorbate.

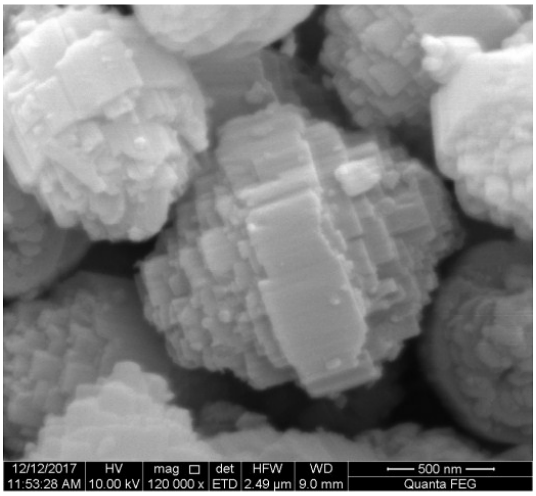

Fig. S1. SEM image of KL zeolite.

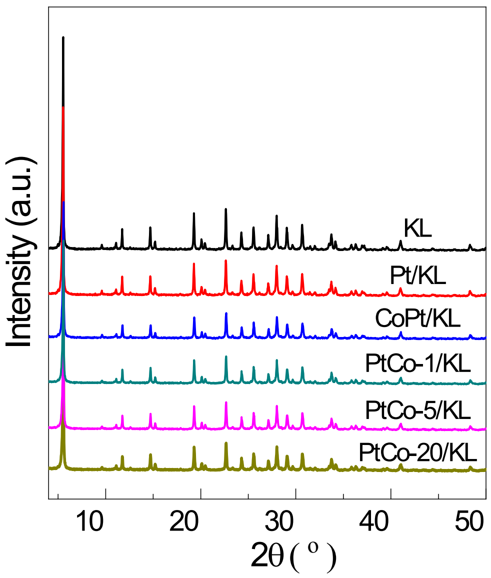

Fig. S2. XRD patterns of catalysts.

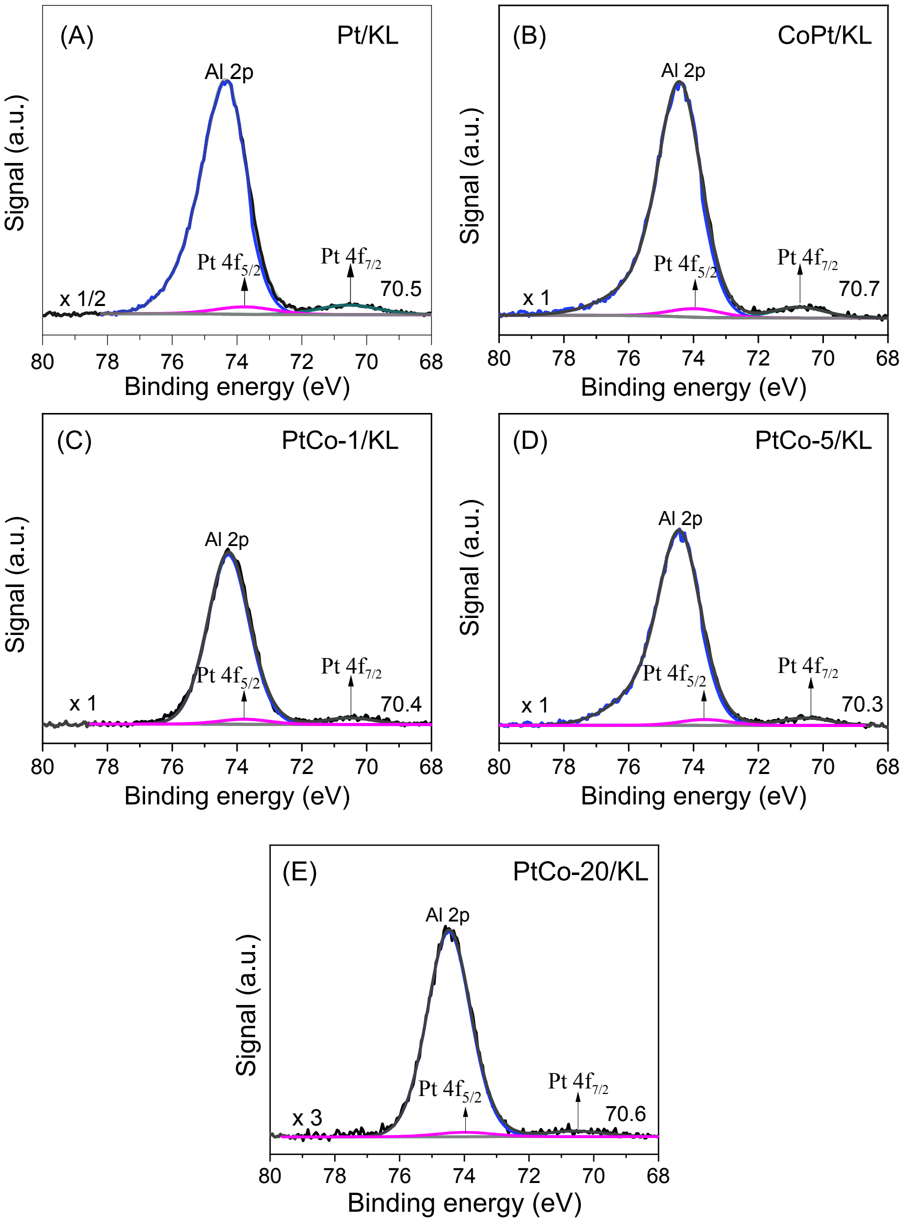

Fig.S3.XPS spectra of Pt4f for the catalysts after H_2 reduction: (A) Pt/KL, (B) CoPt/KL, (C) PtCo-1/KL, (D) PtCo-5/KL and (E) PtCo-20/KL.

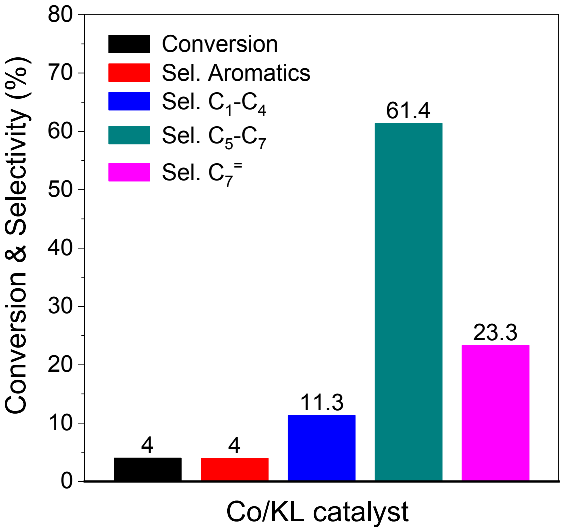

Fig. S4 Catalytic performance of Co/KL catalyst in *n*-heptane aromatization. (Reaction conditions: T = 420 °C, *P* = 0.1 MPa, H_2/*n*-heptane = 6, WHSV = 0.68 h^{-1}).

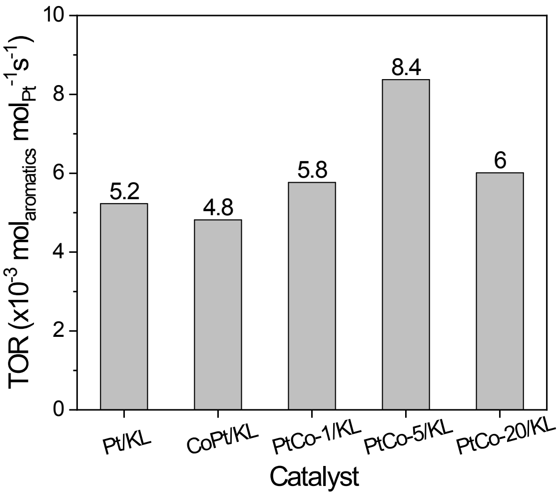

Fig. S5 Turn-over rate (TOR, 10^{-3} mol$_{aromatics}$ mol$_{Pt}^{-1}$ s^{-1}) of *n*-heptane converts to aromatics over catalysts.

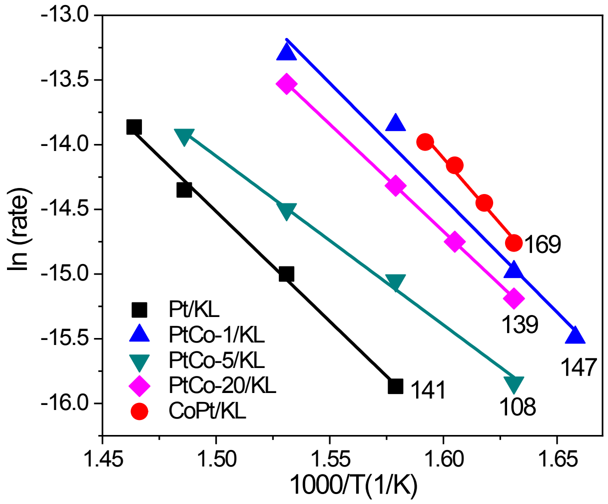

Fig. S6 Arrhenius plots of the catalysts.

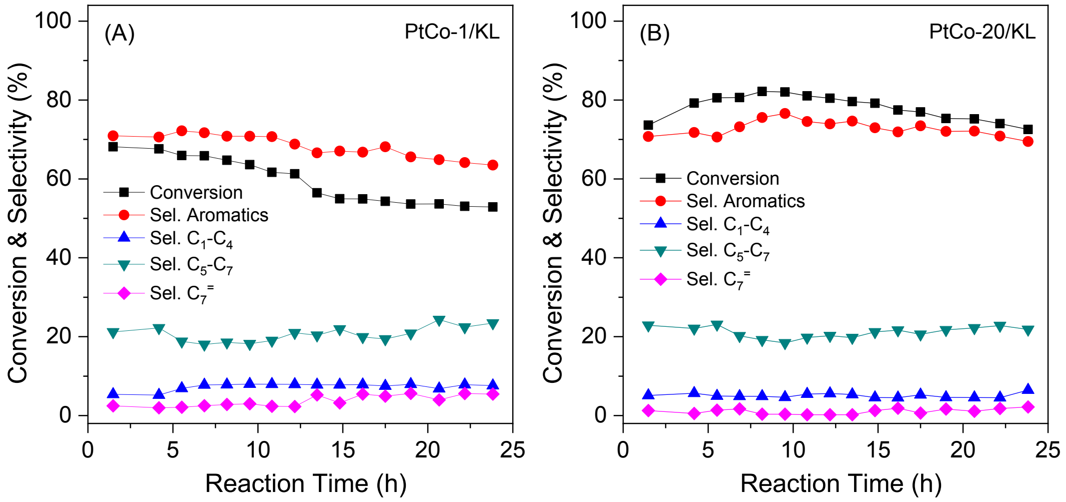

Fig. S7 Catalytic performance of PtCo-1/KL (A), PtCo-20/KL (B) catalysts in *n*-heptane aromatization. (Reaction conditions: T = 420 °C, *P* = 0.1 MPa, H_2/*n*-heptane = 6, WHSV = 0.68 h^{-1}).

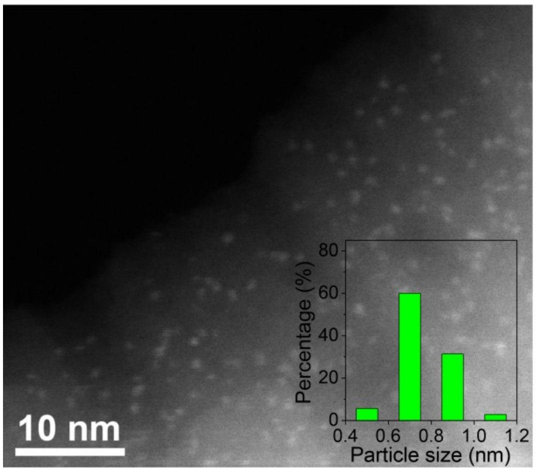

Fig. S8 The STEM images of spent PtCo-5/KL catalyst.

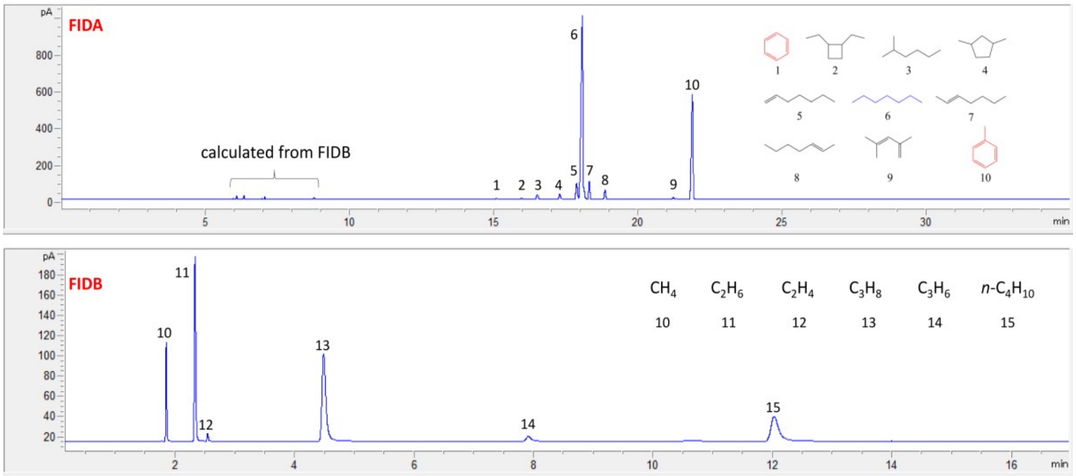

Fig. S9 Typical GC spectroscopy for hydrocarbons in tail gas. (Channel A with flame ionization detector (FIDA): 1: benzene; 2: 1,2-diethylcyclobutane; 3: 2-hexahydrotoluene; 4: 1,3-dimethylcyclopentane; 5: 1-heptene; 6: *n*-heptane;

7-8: 2-heptene; 9: 2,4-dimethylpentene; 10: toluene; Channel B with flame ionization detector (FIDB): 10: methane; 11: ethane; 12: ethylene; 13: propane; 14: propylene; 15: *n*-butane.)

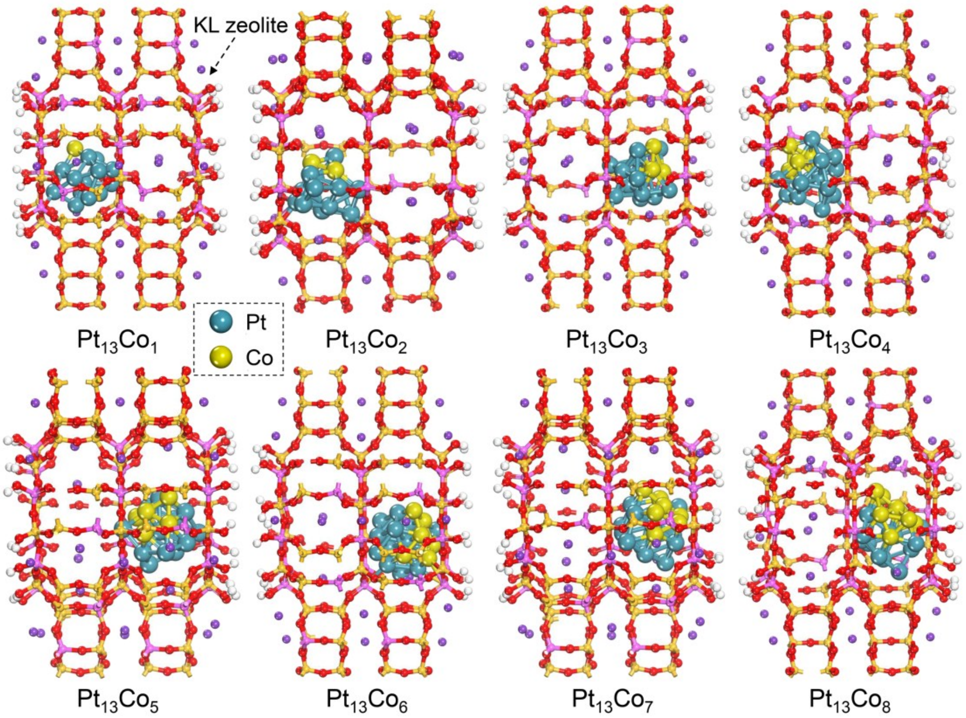

Fig. S10. The DFT calculation models of different Pt-Co clusters.

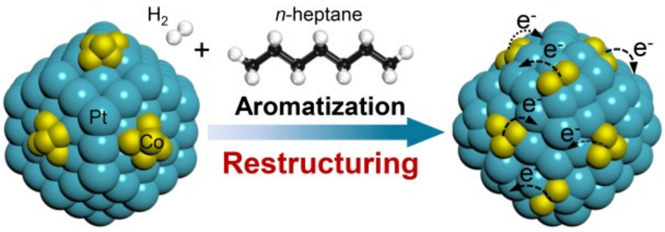

Fig. S11. Restructuring of bimetallic Pt-Co cluster induced by *n*-heptane aromatization.

Table S1 The detailed structural parameters of catalysts.

Sample	Pt[a]	Co[a]	S_{BET} m^2/g	S_{micro}[b] m^2/g^{-1}	S_{exter}[b] m^2/g	V_{micro}[b] cm^3/g	V_{total}[c] cm^3/g
KL	-	-	207	173	34	0.08	0.16
Pt/KL	0.33	-	199	167	32	0.08	0.14
CoPt/KL	0.32	0.03	189	162	27	0.08	0.14
PtCo-1/KL	0.38	0.01	190	165	25	0.08	0.14
PtCo-5/KL	0.35	0.04	192	164	28	0.07	0.13
PtCo-20/KL	0.37	0.10	180	155	25	0.07	0.13

[a] Determined by ICP, “-” means “none”.

[b] Micropore surface areas and micropore volumes were determined by *t*-plot.

[c] Single-point adsorption total pore volumes were evaluated at $P/P_0 = 0.988$.

Table S2 Bader charges of Co atoms in $Pt_{13}Co_x$ (x = 1-8) clusters and the adsorption energy inside KL zeolite channel.

Structure	Bader charge / Co atom								loss electron / Co_{atom}^{-1}	Adsorption Energy of $PtCo_x$ (eV)[a]
Pt_{13}	-								-	-1.42
$Pt_{13}Co_1$	0.32								0.32	0.83
$Pt_{13}Co_2$	0.52	0.61							0.57	-4.66
$Pt_{13}Co_3$	0.55	0.60	0.38						0.51	-3.76
$Pt_{13}Co_4$	0.41	0.50	0.22	0.45					0.40	-3.67
$Pt_{13}Co_5$	0.41	0.37	0.31	0.54	0.23				0.37	-1.83
$Pt_{13}Co_6$	0.37	0.43	0.24	0.37	0.28	0.30			0.33	-2.01
$Pt_{13}Co_7$	0.41	0.38	0.18	0.41	0.17	0.23	0.11		0.27	-1.36
$Pt_{13}Co_8$	0.40	0.37	0.13	0.38	0.12	0.22	0.22	0.03	0.23	0.81

[a] Determined by DFT calculations

Table S3 Detailed results of kinetic study.

Catalyst	T (^{o}C)	Conversion (%)	Reaction rate ($\times10^{-7}$ mol g_{cat}^{-1} s^{-1})
Pt/KL	410	11.4	9.52
	400	7.0	5.81
	380	3.7	3.04
	360	1.5	1.28
CoPt/KL	355	11.6	13.1
	350	10.2	11.5
	345	6.2	5.06
	340	5.5	3.88
PtCo-1/KL	380	14.7	16.7
	360	8.7	9.69
	340	4.9	5.39
	330	1.6	1.73
PtCo-5/KL	400	11.1	9.51
	380	6.1	5.05
	360	3.5	2.9
	340	1.6	1.32
PtCo-20/KL	380	11.9	13.3
	360	5.5	6.06
	350	3.5	3.89
	340	2.3	2.53

Table S4 Parameters used in the Mears' criterion for heat transfer in *n*-heptane aromatization.

paramers	Pt/KL	CoPt/KL	PtCo-1/KL	PtCo-5/KL	PtCo-20/KL
observed benzene rate: $-r_{A(obs)}$ (kmol kg_{cat}^{-1} s^{-1})	1.28×10^{-7}	1.87×10^{-7}	1.32×10^{-7}	2.53×10^{-7}	3.89×10^{-7}
catalyst bed density: ρ_b (kg/m^3)	989	989	989	989	989
catalyst particle radius: R_p (m)	3.35×10^{-4}	3.35×10^{-4}	3.35×10^{-4}	3.35×10^{-4}	3.35×10^{-4}
activation energy: E (kJ/kmol)	1.41×10^{5}	1.69×10^{5}	1.47×10^{5}	1.08×10^{5}	1.39×10^{5}
heat transfer coefficient between gas and pellet: h (J/m^2·s·K)	2.94×10^{3}	2.87×10^{3}	2.89×10^{3}	2.89×10^{3}	2.89×10^{3}
gas constant: R_g (kJ/mol·K)	8.315×10^{-3}	8.315×10^{-3}	8.315×10^{-3}	8.315×10^{-3}	8.315×10^{-3}
reaction temperature: T (K)	633.15	603.15	613.15	613.15	613.15
Reynolds number (Re)	2.73×10^{-4}	2.93×10^{-4}	2.86×10^{-4}	2.86×10^{-4}	2.86×10^{-4}
viscosity: μ (kg/m·s)	2.59×10^{-5}	2.53×10^{-5}	2.55×10^{-5}	2.55×10^{-5}	2.55×10^{-5}
fluid density: ρ (kg/m^3)	3.88×10^{-2}	4.07×10^{-2}	4.0×10^{-2}	4.0×10^{-2}	4.0×10^{-2}
collision integrals: Ω_μ	0.76	0.76	0.76	0.76	0.76
collision diameter: σ (Å)	2.2	2.2	2.2	2.2	2.2
thermal conductivity: h (J/m^2·s·K)	2.94×10^{3}	2.87×10^{3}	2.89×10^{3}	2.89×10^{3}	2.89×10^{3}
heat capacity: $\tilde{C}_p$(J/mol·K)	7.11	7.11	7.11	7.11	7.11
Estimated Mears' criterion: C_M	7.18×10^{-8}	1.42×10^{-7}	8.36×10^{-8}	1.18×10^{-7}	2.33×10^{-7}

The absence of heat transfer was checked by Mears' criterion (C_M). [6, 7]

$$C_M = \left| \frac{-\Delta H r_{obs} \rho_b R_p E}{h T^2 R_g} \right|$$

Where ΔH = heat of reaction (for $C_7H_{16} \rightarrow C_7H_8 + 4H_2$)

r_{obs} = observed reaction rate, kmol/kg_{cat}·s

ρ_b = density of catalyst bed, kg/m^3

R_p = catalyst particle radius, m

E = activation energy, kJ/mol

h = heat transfer coefficient between gas and pellet, J/m^2·s·K

R_g = gas constant, kJ/mol·K

T = reaction temperature, K

In the current work, a gas flow rate of 10.72 ml min^{-1} and a catalyst particle size of 0.25-0.42 mm were employed for the kinetic study. And the concentration of *n*-heptane employed in the feed was 14.29 %.

First, the Reynolds number (Re) is calculated according to the followed formula:

$$Re = \frac{U\rho d_p}{\mu}$$

Where U = free-stream velocity, m/s

ρ = fluid density, kg/m^3

d_p =diameter of pellet, m

μ = viscosity, kg/m·s

The viscosity is calculated according to the following formula:

$$\mu = (2.6693 \times 10^{-5})\frac{\sqrt{MT}}{\sigma^2 \Omega_\mu}$$

Where M = molecular weight, g/mol

T = temperature, K

σ = collision diameter, Å

Ω_μ = collision integrals for use with the Lennard-Jones potential

Since Re << 1, heat transfer coefficient was estimated by assuming Nu (Nusselt number = h×d_p/k_t) = 2, then:

$$Nu = \frac{hd_p}{k_t} \approx 2$$

Where h = heat transfer coefficient, J/m^2·s·K or Watts/m^2·K

d_p = diameter of pellet, m

k_t = thermal conductivity, J/K·m·s

For H_2, the k_t is calculated using the following formula:

$$k_t = (\tilde{C}_p + \frac{4}{5}R_g) \times \frac{\mu}{M}$$

Where R_g = universal gas constant, cal/mol·K

μ = viscosity, kg/m·s

$\tilde{C}_p$ = heat capacity J/mol·K

(1) For the Pt/KL catalyst,

T = 633.15 K

Re = 2.73×10^{-4}

μ = 2.59×10^{-5} kg/m·s

k_t = 0.49 J/K·m·s

$\Delta H = 234.6$ kJ/mol (for $C_7H_{16} \rightarrow C_7H_8 + 4H_2$)

$r_{obs} = 1.28\times10^{-7}$ kmol/kg$_{cat}\cdot$s

$\rho_b = 989$ kg/m^3

$R = 1.68\times10^{-4}$ m

$E = 1.41\times10^{5}$ kJ/kmol

$h = 2.94\times10^{3}$ J/m$^2\cdot$s$\cdot$K

$R_g = 8.3145\times10^{-3}$ kJ/mol$\cdot$K

$$\left|\frac{-\Delta H r_{obs}\rho_b R E}{h T^2 R_g}\right|$$

= [(234.6 kJ/mol)×(1.28×10^{-7} kmol/kg$_{cat}\cdot$s)×(989 kg/m^3)×(1.68×10^{-4} m)×(1.41×10^{5} kJ/kmol)] /

[(2.94×10^{3} J/m$^2\cdot$s$\cdot$K)×(633.15 K)^2×(8.3145×10^{-3} kJ/mol$\cdot$K)]

= $7.18\times10^{-8} < 0.15$

(2) For the CoPt/KL catalyst,

$T = 603.15$ K

$r_{obs} = 1.87\times10^{-7}$ kmol/kg$_{cat}\cdot$s

$E = 1.69\times10^{5}$ kJ/kmol

$h = 2.87\times10^{3}$ J/m$^2\cdot$s$\cdot$K

$$\left|\frac{-\Delta H r_{obs}\rho_b R E}{h T^2 R_g}\right|$$

= [(234.6 kJ/mol)×(1.87×10^{-7} kmol/kg$_{cat}\cdot$s)×(989 kg/m^3)×(1.68×10^{-4} m)×(1.69×10^{5} kJ/kmol)] /

[(2.87×10^{3} J/m$^2\cdot$s$\cdot$K)×(603.15 K)^2×(8.3145×10^{-3} kJ/mol$\cdot$K)]

= $1.42\times10^{-7} < 0.15$

(3) For the PtCo-1/KL catalyst,

$T = 613.15$ K

$r_{obs} = 1.32\times10^{-7}$ kmol/kg$_{cat}\cdot$s

$E = 1.47\times10^{5}$ kJ/kmol

$h = 2.89\times10^{3}$ J/m^{2}·s·K

$$\left|\frac{-\Delta H r_{obs} \rho_b R E}{h T^{2} R_g}\right|$$

= [(234.6 kJ/mol)×(1.32×10^{-7} kmol/kg$_{cat}$·s)×(989 kg/m^{3})×(1.68×10^{-4} m)×(1.47×10^{5} kJ/kmol)] /

[(2.89×10^{3} J/m^{2}·s·K)×(613.15 K)^{2}×(8.3145×10^{-3} kJ/mol·K)]

= $8.36\times10^{-8} < 0.15$

(4) For the PtCo-5/KL catalyst,

$T = 613.15$ K

$r_{obs} = 2.53\times10^{-7}$ kmol/kg$_{cat}$·s

$E = 1.08\times10^{5}$ kJ/kmol

$h = 2.89\times10^{3}$ J/m^{2}·s·K

$$\left|\frac{-\Delta H r_{obs} \rho_b R E}{h T^{2} R_g}\right|$$

= [(234.6 kJ/mol)×(2.53×10^{-7} kmol/kg$_{cat}$·s)×(989 kg/m^{3})×(1.68×10^{-4} m)×(1.08×10^{5} kJ/kmol)] /

[(2.89×10^{3} J/m^{2}·s·K)×(613.15 K)^{2}×(8.3145×10^{-3} kJ/mol·K)]

= $1.18\times10^{-7} < 0.15$

(5) For the PtCo-20/KL catalyst,

$T = 613.15$ K

$r_{obs} = 3.89\times10^{-7}$ kmol/kg$_{cat}$·s

$E = 1.39\times10^{5}$ kJ/kmol

$h = 2.89\times10^{3}$ J/m^{2}·s·K

$$\left|\frac{-\Delta H r_{obs} \rho_b R E}{h T^{2} R_g}\right|$$

= [(234.6 kJ/mol)×(3.89×10^{-7} kmol/kg$_{cat}$·s)×(989 kg/m^{3})×(1.68×10^{-4} m)×(1.39×10^{5} kJ/kmol)] /

[(2.89×10^{3} J/m^{2}·s·K)×(613.15 K)^{2}×(8.3145×10^{-3} kJ/mol·K)]

= $2.33\times10^{-7} < 0.15$

Therefore, heat transfer effect during the kinetic experiment could be neglected

Table S5 Parameters used in the Weisz-Prater Criterion (C_{WP}) for internal mass transfer limitations in *n*-heptane aromatization.

paramers	Pt/KL	CoPt/KL	PtCo-1/KL	PtCo-5/KL	PtCo-20/KL
observed benzene rate: $-r_{A(obs)}$ (mol kg_{cat}^{-1} s^{-1})	1.28×10^{-4}	1.87×10^{-4}	1.32×10^{-4}	2.53×10^{-4}	3.89×10^{-4}
density of catalyst bed: ρ_c (kg/m^3)	1413	1413	1413	1413	1413
catalyst particle radius: R_p (m)	3.35×10^{-4}	3.35×10^{-4}	3.35×10^{-4}	3.35×10^{-4}	3.35×10^{-4}
pressure of *n*-heptane: P_{hep} (atm)	0.143	0.143	0.143	0.143	0.143
Boltzmann'n contant: k_b (J/K)	1.38×10^{-5}	1.38×10^{-5}	1.38×10^{-5}	1.38×10^{-5}	1.38×10^{-5}
gas constant: R_g (atm·cm^3/mol·K)	82.06	82.06	82.06	82.06	82.06
reaction temperature: T (K)	633.15	603.15	613.15	613.15	613.15
molecular diameter: σ_d (cm)	4.3×10^{-8}	4.3×10^{-8}	4.3×10^{-8}	4.3×10^{-8}	4.3×10^{-8}
gas concentration of n-heptane at the external surface of the catalyst: C_s (mol/m^3)	2.75	2.89	2.84	2.84	2.84
effective diffusivity: D_e (m^2/s)	7.93×10^{-8}	7.74×10^{-8}	7.81×10^{-8}	7.81×10^{-8}	7.81×10^{-8}
Weisz-Prater Criterion: C_{WP}	2.34×10^{-2}	3.33×10^{-2}	2.37×10^{-2}	4.55×10^{-2}	6.99×10^{-2}

The absence of mass transport resistances was checked by Weisz-Prater Criterion (C_{WP}) for Internal Diffusion. [8]

$$C_{WP} = \frac{r_{obs}\rho_c {R_p}^2}{D_e C_s} < 1$$

Where r_{obs} = observed reaction rate, mol/kg_{cat}·s

ρ_c = density of catalyst pellet, kg/m^3

R_p = catalyst particle radius, m

D_e = effective diffusivity, m^2/s

C_s = gas concentration of A at the external surface of the catalyst, mol/m^3.

C_s is gas concentration of A at the external surface of the catalyst in mol/m^3. C_s is calculated according to the following formula: [c]

$$C_s = C_o = \frac{N_{hep}}{V} = \frac{P_{hep}}{R_g T}$$

Where P_{hep} is the pressure of *n*-heptane, atm

T = reaction temperature, K

R_g = universal gas constant, atm·cm^3/mol·K

The average velocity for the *n*-heptane molecular is:

$$\bar{v} = \sqrt{\frac{8k_bT}{\pi m}}$$

Where k_b = Boltzmann'n contant, 1.38×10^{-5} J/K

m = mass of *n*-heptane molecular

The mean free path in the gas phase is:

$$\lambda = \frac{1}{\sqrt{2}\pi\sigma^2\frac{N_{hep}}{V}} = \frac{R_gT}{\sqrt{2}\pi{\sigma_d}^2P_{hep}}$$

Where σ_d = molecular diameter, 4.3×10^{-8} cm

The pore diameter is 0.65 nm (from BJH desorption branch), which is much less than the mean free path (λ). Consequently, pore diffusion will be dominated by Knudsen diffusion and

$D_e \approx D_{Kn}$ ($D_{Kn} = \frac{\bar{v}d_{pd}}{3}$)

(1) For the Pt/KL catalyst,

$r_{obs} = 1.28\times10^{-4}$ mol/kg$_{cat}$·s

$\rho_c = 1413$ kg/m^3

$R_p = 1.68\times10^{-4}$ m

$D_e = 7.93\times10^{-8}$ m^2/s

$C_s = 2.75$ mol/m^3.

$$C_{WP} = \frac{r_{obs}\rho_c{R_p}^2}{D_eC_s}$$

= [(1.28×10^{-4} mol/kg$_{cat}$·s) × (1413 kg/m^3) × (1.68×10^{-4} m)^2] / [(7.93×10^{-8} m^2/s)·× (2.75 mol/m^3)]

= 0.023 < 1

(2) For the CoPt/KL catalyst,

$r_{obs} = 1.87\times10^{-4}$ mol/kg$_{cat}$·s

$D_e = 7.74\times10^{-8}$ m^2/s

$C_s = 2.89$ mol/m^3.

$$C_{WP} = \frac{r_{obs}\rho_c {R_p}^2}{D_e C_s}$$

= [(9.71×10^{-4} mol/kg$_{cat}$·s) × (1413 kg/m^3) × (1.68×10^{-4} m)^2] / [(7.74×10^{-8} m^2/s)·× (2.89 mol/m^3)]

= 0.033 < 1

(3) For the PtCo-1/KL catalyst,

r_{obs} = 1.32×10^{-4} mol/kg$_{cat}$·s

D_e = 7.81×10^{-8} m^2/s

C_s = 2.84 mol/m^3.

$$C_{WP} = \frac{r_{obs}\rho_c {R_p}^2}{D_e C_s}$$

= [(8.25×10^{-4} mol/kg$_{cat}$·s) × (1413 kg/m^3) × (1.68×10^{-4} m)^2] / [(7.81×10^{-8} m^2/s)·× (2.84 mol/m^3)]

= 0.024 < 1

(4) For the PtCo-5/KL catalyst,

r_{obs} = 2.53×10^{-4} mol/kg$_{cat}$·s

D_e = 7.81×10^{-8} m^2/s

C_s = 2.84 mol/m^3.

$$C_{WP} = \frac{r_{obs}\rho_c {R_p}^2}{D_e C_s}$$

= [(6.86×10^{-4} mol/kg$_{cat}$·s) × (1413 kg/m^3) × (1.68×10^{-4} m)^2] / [(7.81×10^{-8} m^2/s)·× (2.84 mol/m^3)]

= 0.046 < 1

(5) For the PtCo-20/KL catalyst,

r_{obs} = 3.89×10^{-4} mol/kg$_{cat}$·s

D_e = 7.81×10^{-8} m^2/s

C_s = 2.84 mol/m^3

$$C_{WP} = \frac{r_{obs}\rho_c {R_p}^2}{D_e C_s}$$

$= [(6.86\times10^{-4}\ \mathrm{mol/kg_{cat}\cdot s}) \times (1413\ \mathrm{kg/m^3}) \times (1.68\times10^{-4}\ \mathrm{m})^2] / [(7.81\times10^{-8}\ \mathrm{m^2/s})\cdot\times (2.84\ \mathrm{mol/m^3})]$

$= 0.07 < 1$

Therefore, internal diffusion effect could be neglected during the kinetic experiments.

Table S6 Parameters used in the Mears' Criterion (C_{MR}) for estimating external mass transfer limitations in *n*-heptane aromatization.

paramers	Pt/KL	CoPt/KL	PtCo-1/KL	PtCo-5/KL	PtCo-20/KL
observed benzene rate: $-r_{A(obs)}$ (mol kg_{cat}^{-1} s^{-1})	1.28×10^{-4}	1.87×10^{-4}	1.32×10^{-4}	2.53×10^{-4}	3.89×10^{-4}
density of catalyst bed: ρ_c (kg/m^3)	1413	1413	1413	1413	1413
catalyst particle radius: R_p (m)	3.35×10^{-4}	3.35×10^{-4}	3.35×10^{-4}	3.35×10^{-4}	3.35×10^{-4}
reaction order	0.6	0.6	0.6	0.6	0.6
gas constant: R_g (atm·cm^3/mol·K)	82.06	82.06	82.06	82.06	82.06
reaction temperature: T (K)	633.15	603.15	613.15	613.15	613.15
binary diffusion coefficient: D_{AB} (m^2/s)	1.11×10^{-4}	1.02×10^{-4}	1.05×10^{-4}	1.05×10^{-4}	1.05×10^{-4}
Lennard-Jones parameter: σ_{AB} (Å)	4.79	4.79	4.79	4.79	4.79
external mass transfer coefficient: k_c (m/s)	0.66	0.61	0.63	0.63	0.63
bulk gas concentration of *n*-heptane: C_{AB} (mol/m^3)	2.55	2.55	2.55	2.55	2.55
Nusselt number: Sh	~2	~2	~2	~2	~2
Mears' Criterion: C_{MR}	3.58×10^{-5}	5.69×10^{-5}	3.90×10^{-5}	7.48×10^{-5}	1.15×10^{-4}

The absence of mass transport resistances was checked by Mears' Criterion (C_{MR}) for External Diffusion. [6, 9]

$$C_{MR} = \frac{r_{obs}\rho_c R_p n}{k_c C_{AB}} < 0.15$$

Where r_{obs}= observed reaction rate, mol/kg_{cat}·s

ρ_c = density of catalyst pellet, kg/m^3

R_p = catalyst particle radius, m

n = reaction order

k_c = external mass transfer coefficient, m/s

C_{AB} = bulk gas concentration of A, mol/m^3

For the H_2-*n*-heptane system, the diffusion coefficient of *n*-heptane is calculated based on the following formula: [2]

$$D_{AB} = 0.001853 \times \sqrt{T^3\left(\frac{1}{M_A}+\frac{1}{M_B}\right)} \times \frac{1}{P{\sigma_{AB}}^2\Omega_{D_{AB}}}$$

$$\Omega_{D_{AB}} = \frac{1.06036}{T^{*\,0.15610}} + \frac{0.193}{e^{0.47635 \cdot T^{*}}} + \frac{1.03578}{e^{1.52996 \cdot T^{*}}} + \frac{1.76474}{e^{3.89411 \cdot T^{*}}}$$

Where D_{AB} = binary diffusion coefficient of A in B, m^2/s

ϕ_p = pellet porosity

σ_c = constriction factor

$\tilde{\tau}$ = tortuosity

M_A = molecular weight of H_2, g/mol

M_B = molecular weight of *n*-heptane, g/mol

P = reaction pressure, atm

σ_{AB} = Lennard-Jones parameter, Å

Ω_{AB} = collision Integral

T^* = $\frac{kT}{\varepsilon}$

Because Re << 1, the Nusselt number ($Sh = 2 + 0.6Re^{1/2}Sc^{1/3}$) can be estimated to be 2 (Sc is Schmidt number, $Sc = \frac{v}{D_{AB}}$). Then,

$$Sh = \frac{k_c \times d_p}{D_{AB}} \approx 2$$

Where k_c = external mass transfer coefficient, m/s

d_p = diameter of pellet, m

(1) For the Pt/KL catalyst,

r_{obs}= 1.28×10^{-4} mol/kg_{cat}·s

ρ_c = 1413 kg/m^3

R_p = 1.68×10^{-4} m

n = 0.6

k_c = 0.66 m/s

C_{AB} = 2.55 mol/m^3

$$\frac{r_{obs}\rho_c R_p n}{k_c C_{Ab}}$$

= [(1.28×10^{-4} mol/kg_{cat}·s) × (1413 kg/m^3) × (1.68×10^{-4} m)^2 × 0.6] / [(0.66 m/s)·× (2.55 mol/m^3]

= $3.58\times10^{-5} < 0.15$

(2) For the CoPt/KL catalyst,

r_{obs}= 1.87×10^{-4} mol/kg$_{cat}$·s

k_c = 0.61 m/s

C_{AB} = 2.55 mol/m^3

$$\frac{r_{obs}\rho_c R_p n}{k_c C_{Ab}}$$

= [(1.87×10^{-4} mol/kg$_{cat}$·s) × (1413 kg/m^3) × (1.68×10^{-4} m)^2 × 0.6] / [(0.61 m/s)·× (2.55 mol/m^3]

= $5.69\times10^{-5} < 0.15$

(3) For the PtCo-1/KL catalyst,

r_{obs}= 1.32×10^{-4} mol/kg$_{cat}$·s

k_c = 0.63 m/s

C_{AB} = 2.55 mol/m^3

$$\frac{r_{obs}\rho_c R_p n}{k_c C_{Ab}}$$

= [(1.32×10^{-4} mol/kg$_{cat}$·s) × (1413 kg/m^3) × (1.68×10^{-4} m)^2 × 0.6] / [(0.63 m/s)·× (2.63 mol/m^3]

= $3.9\times10^{-5} < 0.15$

(4) For the PtCo-5/KL catalyst,

r_{obs}= 2.53×10^{-4} mol/kg$_{cat}$·s

k_c = 0.63 m/s

C_{AB} = 2.55 mol/m^3

$$\frac{r_{obs}\rho_c R_p n}{k_c C_{Ab}}$$

= [(2.53×10^{-4} mol/kg$_{cat}$·s) × (1413 kg/m^3) × (1.68×10^{-4} m)^2 × 0.6] / [(0.63 m/s)·× (2.55 mol/m^3]

= $7.48\times10^{-5} < 0.15$

(5) For the PtCo-20/KL catalyst,

r_{obs}= 3.89×10^{-4} mol/kg$_{cat}$·s

$k_c = 0.63$ m/s

$C_{AB} = 2.55$ mol/m^3

$$\frac{r_{obs}\rho_c R_p n}{k_c C_{Ab}}$$

$= [(3.89\times10^{-4}\ \text{mol/kg}_{\text{cat}}\cdot\text{s}) \times (1413\ \text{kg/m}^3) \times (1.68\times10^{-4}\ \text{m})^2 \times 0.6] / [(0.63\ \text{m/s})\cdot\times (2.55\ \text{mol/m}^3]$

$= 1.15\times10^{-4} < 0.15$

Therefore, external diffusion effect could be neglected during the kinetic experiments.

References:

[1] G. Kresse and J. Furthmüller, *Comp. Mater. Sci.*, 1996, **6**, 15−50.

[2] G. Kresse and J. Furthmüller, *Phys. Rev. B*, 1996, **54**, 11169−11186.

[3] G. Kresse and D. Joubert, *Phys. Rev. B*, 1999, **59**, 1758−1775.

[4] P. E. Blöchl, *Phys. Rev. B*, 1994, **50**, 17953−17979.

[5] J. P. Perdew, K. Burke and M. Ernzerhof, *Phys. Rev. Lett.*, 1996, **77**, 3865−3868.

[6] H.S. Fogler, Elements of Chemical Reaction Engineering, 5th ed, Prentice Hall, Upper Saddle River, NJ, 2016.

[7] R.B. Bird, W.E. Stewart, and E.N. Lightfoot, Transport Phenomena, 2nd Edition, John Wiley & Sons, Inc, 605 Third Avenue, New York, 2002.

[8] M. Albert Vannice, Kinetics of Catalytic Reactions, Springer Science + Business Media, Inc., 233 Spring Street, New York, NY 10013, USA, 2005.

[9] W. S. Lee, Z. Wang, R. J. Wu, A. Bhan, *J. Catal.* 2014, **319**, 44-53.